Christopher Lenz*, Finja Borowski, Jan Oldenburg, Christoph Brandt-Wunderlich, Michael Stiehm and Klaus-Peter Schmitz

Flow analysis of steady state forward flow of aortic valve prostheses using Particle Image Velocimetry

https://doi.org/10.1515/cdbme-2024-2103

Abstract: Transcatheter aortic valve replacement (TAVR) has become the standard therapy for aortic valve stenosis in patients with high surgical risk. Understanding the flow dynamics in TAVR is crucial for its evaluation and optimization. Experimental flow measurement by means of Particle Image Velocimetry (PIV) is increasingly applied alongside numerical analyses.

This study introduces a novel test rig concept enabling the determination of velocity fields using Stereo-PIV under steady forward flow conditions through a TAVR during the peak systole matching the ISO 5840-1:2021 requirements. The experimental setup utilized an impeller pump to generate steady forward flow through a silicone aortic root model with implanted TAVR. A Stereo-PIV setup captured velocity fields in both ventricular inflow and aortic outflow regions. Test conditions were based on physiological flow rates determined from pulsatile measurements. Illumination of the added particles in the test fluid was achieved using an Nd:YAG laser. Fluorescent polystyrol particles (size: 50 µm) were used for flow visualization.

Results showed characteristic flow patterns: a central jet flow entering the TAVR in the ventricular flow field. A jet flow directed towards the sinus side and a recirculation zone forming on the opposite side of the sinus could be detected in the aortic outflow. The width of the recirculation zone increases with distance from the TAVR. Maximum flow velocities were detected at 0.78 m/s for the ventricular flow field and 0.94 m/s for the aortic flow field.

This study provides a comprehensive approach for fluid dynamic analysis of TAVR under steady flow conditions, offering insights into flow mechanics performance crucial for device optimization. Further investigations could enhance the PIV – measurement procedure by increasing both the spatial resolution and the tracer particle density within the acquired images for a comprehensive characterization of TAVR flow dynamics.

Keywords: particle image velocimetry, steady forward flow, TAVR

1 Introduction

In the past, the minimally invasive implantation of transcatheter aortic valve replacement (TAVR) was established as the standard therapy for patients with high surgical risk in the treatment of aortic valve stenosis [1]. In order to investigate the general flow behaviour of TAVR and to evaluate and optimize the fluid dynamic performance of TAVR, *in vitro* measurement techniques such as Particle Image Velocimetry (PIV) are increasingly being used alongside numerical flow analyses [2, 3].

The ISO 5840-1:2021 mandates the use of Particle Image Velocimetry (PIV) for the flow analysis of TAVR in terms of the thrombotic risk [4]. Additionally, within ISO 5840-1:2021, various possible physiological testing scenarios are listed. One of these scenarios is the fluid analysis using a steady forward flow through the TAVR being tested [4]. The steady forward flow can be analogously described as the moment of peak systolic within the cardiac cycle [5, 6]. To the best of the authors knowledge, there are no published studies concerning the fluid analysis of a TAVR using Stereo-PIV under the implementation of steady forward flow condition in the relevant literature. Therefore, within this study, a test rig concept was developed enabling the determination of velocity-fields using Stereo-PIV during steady flow conditions through a TAVR. The motivation of this study was to identify characteristic flow properties such as the distribution of velocity fields, occurring fluid dynamic phenomena such as turbulence, or the circular propagation of the flow field.

The presented test setup is primarily intended to investigate the fluid dynamic processes during peak systole. This allows a fluid dynamic characterization of TAVR to be determined and design-related optimization approaches to be derived. Furthermore the results could serve as validation test case for further *in silico* investigations of TAVR flow.

Corresponding author: Christopher Lenz:
Institute for ImplantTechnology and Biomaterials e.V., Friedrich-Barnewitz-Str. 4, 18119 Rostock-Warnemuende, Germany,
e-mail: christopher.lenz@iib-ev.de
Finja Borowski, Jan Oldenburg, Christoph Brandt-Wunderlich, Michael Stiehm, Klaus-Peter Schmitz:
Institute for ImplantTechnology and Biomaterials e.V., Rostock-Warnemuende, Germany

2 Materials and Methods

2.1 Experimental setup and test bench concept

The steady forward flow was generated by an impeller pump, which continuously circulates the fluid Figure 1. A heat exchanger, temperatured the test fluid to a temperature of 37±2°C. A bypass system was implemented to regulate the flow rate in the pump circuit.

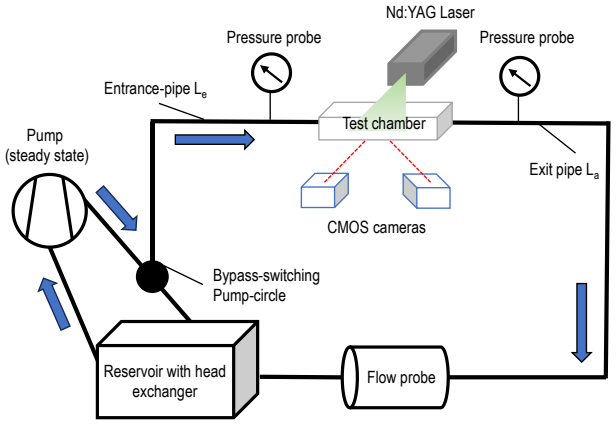

Figure 1: Schematic representation of the test setup. The bypass-switch directs the corresponding flow rate from the continuous pumping circuit to the test section

To fulfil the objective of a test bench for steady state forward flow measurements using Stereo-PIV, a custom made test chamber made of PMMA was developed. The length of the viewing windows for the cameras was dimensioned to provide the widest possible measurement field (in the *y*-direction), allowing for the analysis of both the aortic region (distal to the TAVR to be measured/ outflow area) and the ventricular region (proximal to the TAVR to be measured/ inflow area) within a single measurement setup, including calibration. The chamber was mounted on a horizontal tabletop. Figure 2 shows the test chamber with the flow direction (inlet and outlet) marked by the blue arrows passing through the chamber.

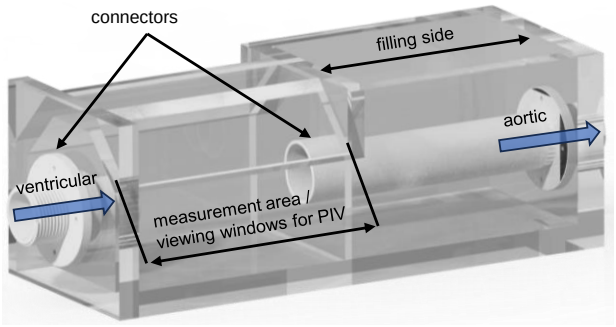

Figure 2: Test chamber with inserted connectors for the aortic root model (blue arrows show flow direction)

Pressure sensors were placed proximal and distal the test chamber to determine the pressure gradient across the TAVR. At the end of the test section, a flow sensor was integrated.

The TAVR was implanted into a silicone aortic root model as described in a prior study [2]. The aortic root model was made of transparent silicone (Sylgard 184 Silicone Elastomer; The Dow Chemical Company, Midland, MI, USA). The molds for the silicone model were produced using 3D printing techniques (Objet30, Stratasys Ltd., Rechovot, Israel). Both the TAVR and the aortic root model were placed inside the test chamber [2].

The camera viewing windows were tilted by 45° relative to the light sheet plane, allowing both PIV cameras an orthogonal view. The ratio of the test fluid was adjusted to achieve a kinematic viscosity of ν = 3.5 cSt. In addition, the refractive index of the test fluid almost corresponded to the refractive index of silicone. As a result of the refractive index adjustment, the distortion induced by the silicone model was minimized.

To ensure optical access to the TAVR flow without distortion, the test chamber was also filled with test medium. Thus, the entire aortic root model was surrounded by the test medium and simultaneously flowed through by the system volume flow rate. For PIV measurement, after filling the chamber, a lid was tightly screwed onto the open filling side.

2.2 PIV setup and flow conditions

A Stereo-PIV setup from Dantec Dynamics (Skovlunde, DEN) was arranged around the chamber, consisting of two cameras, a laser sheet optic, and a laser. The camera system for the Stereo-PIV setup comprised two CMOS cameras (EoSens 12CXP+, 8-bit, Mikrotron, Germany), positioned at a relative angle of 45° to the light sheet plane. Illumination of the added particles in the test fluid was achieved using an Nd:YAG laser (Litron Lasers Ltd., England, wavelength: 532 nm, max. pulse energy: 800 mJ, frequency: 15 Hz). Fluorescent polystyrol particles (microParticles GmbH, Germany, size: 50 µm) were used for flow visualization. The particle distribution was captured in double-frame mode and averaged over 200 frames. Additionally, three time intervals between laser pulses were used to accurately capture both high and low velocities (Δt = 260 µs, 500 µs, and 5240 µs). An interrogation area (IA) size of 128 Px^2 (pixel pitch: 7.05 µm/Px) with 50% overlap was utilized for evaluating velocity vectors. Camera calibration was performed using a double-sided point target.

Since the chamber can be moved between the ventricular and aortic measurement fields along the *x*-axis on the test bench, a single calibration for both measurement fields sufficed here. Only the aortic root model with the TAVR was moved during this process. A change in the measurement field

(ventricular to aortic) with respect to the cameras in the *y*- and *z*-directions was realized due to a guided rail system.
For the analysis of the PIV recordings, the images were optimized with various image post-processing steps such as image arithmetic, image masking, gaussian filter, mean filter and grey-value threshold.

In this work, the cardiac output (*CO*) was utilized to derive the scenario to be measured. In order to use forward flow rates for the steady state measurements, flow rates from pulsatile measurements with a pulse duplicator system (ViVitro Inc., Victoria, Canada) were analysed with respect to the flow rate during peak systole. A cardiac output of CO = 2.5 l/min was set at a constant heart rate (f = 70 bpm) using the pulse duplicator system in order to create different measurement scenarios and to derive the corresponding Reynolds numbers (*Re*) (Table 1).

Table 1: overview of the calculated measurement scenarios.

Cardiac Output *CO* [l/min]	Reynolds-Number *Re*	Flow rate *Q* [l/min]	Scenario
2.5	3897.7	16.71	S1

The minimum pipe length (L_e = 0.45 m) for a fully developed flow profile (as required by ISO 5840-1:2021 [4]) was determined with [6]:

$$L_e \approx 4{,}4 \cdot Re^{1/6} \cdot d \qquad (1)$$

To minimize or compensate for flow disturbances before and after the test chamber and to enable further measurement scenarios with a higher *CO* to be measured, the inlet length was chosen as L_e = 1 m and the outlet length as L_a = 0.6 m.

3 Results

In Figure 3 the measurement scenario S1 is shown for the ventricular inflow and for the aortic outflow in the z = 0 mm plane. Within the ventricular inflow, a jet flow was observed at the centre without any recirculation zones. Here, maximum flow velocities of approximately 0.78 m/s were observed at the centre of the jet flow just before entering the TAVR. Towards the wall, flow velocities decreased to below 0.3 m/s. However, this could not be demonstrated by the measurements conducted due measurement errors.

A flat velocity profile with a sharp decrease in velocities towards the edges was formed, with high velocities focussed in the flow centre with increasing distance from the flow inlet or towards the TAVR. Similarly, velocities increased towards the centre of the flow and reach their highest values just before entering the TAVR. The velocity magnitude in Figure 3 shows the expected flow profile, which exhibits a sharp decrease in velocities just before reaching the tube wall (in this case, the wall of the aortic root model).

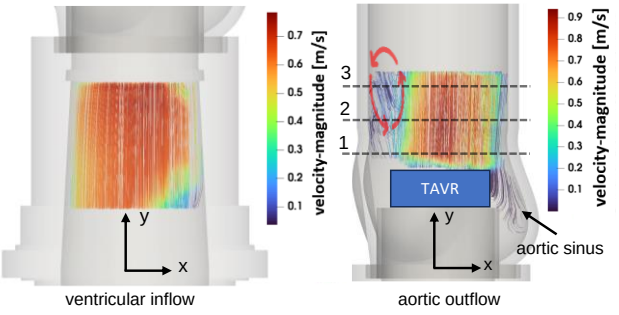

Figure 3: velocity magnitude for the ventricular and aortic flow field in the z = 0 mm plane.

The valve leaflets of the TAVR, behind which the flow enters the aortic root, are schematically indicated by blue rectangles. The aortic flow field is illustrated with local velocity values corresponding to streamlines and color scaling. Additionally, horizontal dashed lines (numbers 1–3) are drawn at various heights of the flow field, based on which further analyses of the flow profiles were conducted.

In the centre of the aortic flow field, a jet with a maximum velocity magnitude of 0.94 m/s was formed. The velocity magnitude decreased towards the vessel walls. A recirculation zone was built on the opposite side of the sinus of the aortic root due to a vortex. This recirculation zone is highlighted in Figure 3 by the red circular arrow. Between the jet flow and the recirculation zone, a transition layer was formed, characterized by a drastic decrease in velocities from the jet to the vortex. This vortex rotated in the mathematically positive direction towards the vessel wall. Additionally, the centre of the vortex seemed to form not immediately behind the valve leaflet but rather further distal to the TAVR. It is evident that the diversion increases with distance from the TAVR or towards the sinus.

The flow changed noticeably when transitioning from the ventricular side to the aortic part of the aortic root. A rapid jet flow with an emerging vortex on the opposite side of the sinus was formed behind the valve leaflet. It is clearly visible how the flow velocity in the centre, distal to the leaflet, increased and focused from the flat profile of the turbulent ventricular inflow region (Figure 3).

Figure 4 highlights again that the width of the recirculation zone increases with distance from the TAVR. While line 1 still shows low negative flow velocities, lines 2 and 3 indicate an increase in velocity components in the negative *y*-direction, suggesting the circulatory nature of the flow.

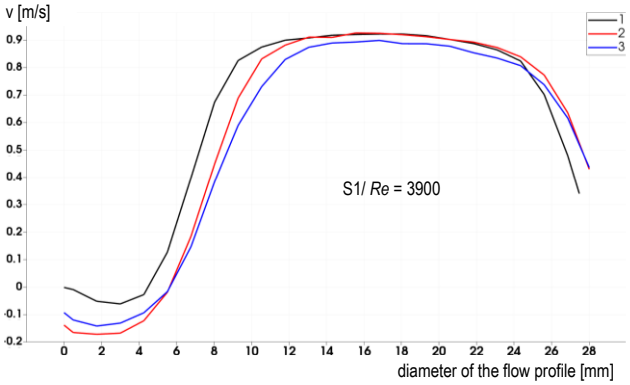

Figure 4: Flow profiles along the main flow direction for S1 as linear interpolation between the individual measurement points of the aortic flow area.

Additionally, it can be seen that within the jet flow region (Figure 4: x-values from 8–28 mm) further distal to the TAVR, such as at line 3, the flat profile of the turbulent flow gradually emerged. For line 3 for example, the jet region is approximately determined on the graph within the range from $12 \leq x \leq 25$ mm. The examination of the flow field in Figure 3 also suggests the spatial diversion of the jet flow by the recirculation zone within the ascending aorta region. The increasing displacement in the *x*-direction of lines 1–3 in Figure 4 indicates this diversion. The jet flow region shifts towards the sinus side, away from the recirculation zone.

The obtained results are consistent with those from the studies by Ducci et al. (2016) and those from Oldenburg et al. (2022) [3, 5].

4 Conclusion

This study provides an approach for measuring velocity fields in TAVR using Stereo-PIV under steady forward flow conditions. Through the setup of the test bench and the application of various analysis methods, velocity fields can be determined under different flow conditions.

With the developed test rig, both the width of the jet flow and length of the recirculation zone can be quantified (Figure 4), allowing for initial assessments of TAVR design before more complex pulsatile *in vitro* studies or *in silico* simulations are conducted. Also, considering that the time investment in this measurement method is significantly lower compared to the others (pulsatile and simulation).

Moving towards the vessel wall, a recirculation region forms on the opposite side of the sinus. The recirculation region appears to form its centre further distal to the TAVR and becomes smaller with increasing flow rate, resulting in a larger diameter of the jet flow. Additionally, a certain deflection (away from the recirculation region) of the jet flow towards the vessel wall on the sinus side can be observed. This deflection also appears to decrease with increasing flow rate in parallel with the diminishing recirculation region. Hence, the degree of flow diversion behind the leaflet towards the vessel wall could be a potential criterion for assessing the flow mechanics performance of TAVR.

It can be concluded that the size of the recirculation region and the deflection and maximum flow velocities of the jet are relevant for the flow mechanical performance of the TAVR, and further for deriving an assessment of the TAVR design or implant geometry. However, to derive more comprehensive information from the velocity fields, further investigations could optimize the PIV – measurement procedure by increase both the spatial resolution and the tracer particle density within the acquired images.

Author Statement

Research funding: This project has received funding from the European Union's Horizon 2020 research and innovation program under grant agreement No 101017578. The EU is not responsible for any use that may be made of the results shown in this publication or any information contained therein. Conflict of interest: Authors state no conflict of interest.

References

[1] Deutsche Herzstiftung, 2021: "Deutscher Herzbericht 2021 – Sektionsübergreifende Versorgungs-analyse zur Kardiologie, Herzchirurgie und Kinderherzmedizin in Deutschland"

[2] Borowski F, Kaule S, Oldenburg J, et al.: „Particle-Image-Velocimetry zur strömungsmechanischen Analyse des thrombogenen Potentials von Transkatheter -Aortenklappenprothesen". In: tm - Technisches Messen 89 (2022), No. 3, pp. 189–200

[3] Ducci, A; Pirisi, F;Tzamtzis, S; Burriesci G: "Transcatheter aortic valves produce unphysiological flows which may contribute to thromboembolic events: An in-vitro study." In: Journal of biomechanics (2016), No. 16, pp. 4080–4089

[4] ISO 5840 - 1. 05 - 2021.: „Cardiovascular implants–Cardiac valve prostheses –Part 1: General requirements"

[5] Oldenburg J, Borowski F, Kaule S, et al.: „Messung des stationären Vorwärtsflusses einer Transkatheter-Aortenklappenprothese mittels Particle Image Velocimetry." In: Fachtagung "Experimentelle Strömungsmechanik"; German Association for Laser Anemometry GALA e.V. (2022)

[6] Silbernagl S, Despopoulos A: „Taschenatlas Physiologie: 201 Farbtafeln von Rüdiger Gay und Astried Rothenburger." 8. ed.: Thieme Stuttgart; New York, 2012

[7] Entrance Length in Fluent: Understanding its Impact on Flow Simulations. URL https://engineerexcel.com/entrance-length-in-fluent/. – date: 2023-04-06